Synthesis of 4-methylthiazol-2(3H)-thione derivatives and their application as corrosion inhibitors: weight loss, electrochemical, XPS and theoretical study

O. Benali, M. Zebida, Ulrich Maschke, A. Attou, S. Bilgiç

Applied Journal of Environmental Engineering Science

Synthesis of 4-methylthiazol-2(3H)-thione derivatives and their application as corrosion inhibitors: weight loss, electrochemical, XPS and theoretical study

O. Benali[a]*, M. Zebida[a], U. Maschke[b], A. Attou[a], S. Bilgiç[c]

[a]*Laboratory of Chemistry: Synthesis, Properties and Applications, University of Saida –Dr. Moulay Tahar, Algeria.*
[b]*Unité Matériaux et Transformations: Ingénierie des systèmes polymères (UMET :ISP), Université Lille1, France*
[c]*Department of Chemistry, Faculty of Science, Ankara University, Ankara, Turkey*

Corresponding author. E-mail : benaliomar@hotmail.com

Received 08 Apr 2021, Revised 21 May 2021, Accepted 03 Jun 2021

Abstract

The corrosion inhibition of C38 steel in 1M HCl by isomeric derivatives of 4-methylthiazol-2(3H)-thione (**TO1, TO4** and **TO6**) has been investigated using weight loss and electrochemical measurements supplementing with surface characterization study using X-ray photoelectron spectroscopy (XPS). Experimental observations were found to be in agreement with density functional theory (DFT) calculations. The inhibition efficiency increases with increase in the three compounds concentration and showed maximum inhibition efficiency of 98.33%, 96.91% and 94.44% for **TO1**, **TO4** and **TO6** at 2.10^{-4}M in HCl 1M, respectively, at concentration of 2×10^{-4} M at 30°C. Polarization curves reveal that the three inhibitors act as mixed type inhibitor with tendency to anodic branch. Impedance parameters (charge transfer resistance, R_t, and double-layer capacitance, C_{dl}) indicate that the investigated compounds form stable protective films on the steel surface. Adsorption of **TO1**, **TO4** and **TO6** on the C38 steel surface is found to obey the Langmuir adsorption isotherm. The X-ray photoelectron spectroscopy (XPS) of the carbon steel treated with the three compounds indicated that these later are chemically adsorbed on the steel surface. Good correlations were obtained between the anti-corrosion performance of these donor-acceptor compounds and their molecular properties.

Keywords: *Corrosion inhibition; C38 steel; 1M HCl; 4-methylthiazol-2(3H)-thione derivatives, XPS*

1. Introduction

Carbon steel is widely used in several (pipe lines, petroleum, and chemical) industries. Carbon steel has many properties which make it of particular interest, among them: high mechanical strength, easy handling with less expensive cost, easy fabrication and low cost [1,2]. Unfortunately, due to this use of importance, it is in frequent contact with corrosive media in different industries [3]. To overcome this problem, it is necessary to find excellent protection methods. The most commonly used one is the use of inhibitors [4–8]. Organic inhibitors containing polar groups have proven to be practically effective inhibitors in different acid solutions [9-11]. In addition, organic inhibitors containing nitrogen (N) are

effective in HCl, while compounds containing sulfur (S) are effective in H_2SO_4. On the other hand, the compounds which contain N and S behave better as corrosion inhibitor for different acids [12-13]. The presence of an inhibitor on the metal surface after adsorption modifies the electrochemical behavior of the metal / medium system by reducing the aggressiveness of the solution.

In continuation [14], this work is focused at synthesizing some isomeric derivatives of 3-(2-methoxyphenyl)-4-methylthiazol-2(3H)-thione **(TO1),** 3-phenyl-4-methylthiazol-2(3H)-thione **(TO4)** and 3-(2-methyl-phenyl)-4-methylthiazol-2(3H)-thione **(TO6)** and studying their inhibition efficiency on carbon steel in 1 M HCl using different methods (weight loss measurement and electrochemical methods). The XPS was used to study the surface morphology of the compounds.

2. Experimental Section

2.1. Materials and solution

The metal used in this study as working electrode or for weight loss experiments was prepared from C38 carbon steel, where the composition, method of preparation and the preparation method of the aggressive solution (1M HCl) was given in our previous published work [14].

2.2. *Corrosion inhibitors*

The synthesis of the different thiazol-2-thione derivatives was carried out according to the methods described in the literature [15-16]. The structures of the obtained compounds are given in Figure 1.

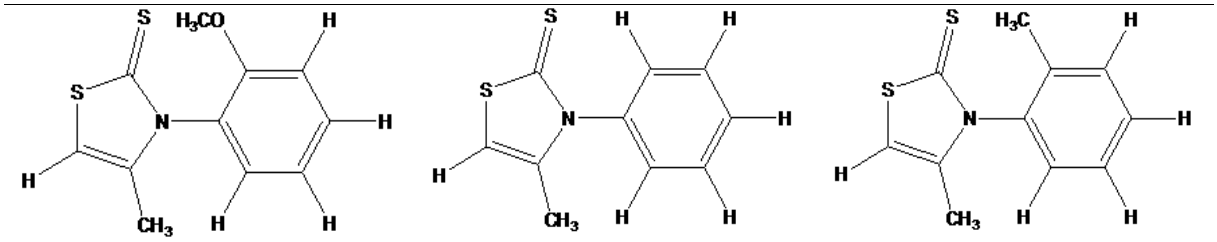

TO1 **TO4** **TO6**

Figure 1. Chemical structures of 4-methylthiazol-2(3H)-thione derivatives

2.3. Experimental methods

The gravimetric and electrochemical measurement protocols as well as the calculation methods were carried out according to what described in our work published previously [14]. The XPS tests were done in the same way as in [14]. The measurements were affected at 30°C after 1 h of immersion of the C38 carbon steel coupons into 100 mL of 1M HCl. The inhibitors are used in various amounts of inhibitors (10^{-6}-2.10^{-4}M).

The structures and electronic properties of **TO1**, **TO4** and **TO6** have been calculated by Gaussian 09W, using the Becke's three-parameter hybrid density functional (DFT) B3LYP method with the standard 6-31G(d,p) [17-18].

3. Results and discussion

3.1. Weight loss measurements

Table 1 lists the corrosion data obtained from this method in the presence of the inhibitors in 1M HCl.

Table 1. Weight loss parameters of **TO1**, **TO4** and **TO6** in 1M HCl solution

Inhibitors	Conc. (M)	C.R. (mg cm^2 h^{-1})	$EI_{C.R.}$ (%)
	Blank	**1.00**	**------**
TO1	10^{-6}	0.61	**39**
	10^{-5}	0.41	**59**
	10^{-4}	0.23	**77**
	2.10^{-4}	0.03	**97**
TO4	5.10^{-6}	0.65	**35**
	10^{-5}	0.43	**57**
	10^{-4}	0.24	**76**
	2.10^{-4}	0.06	**94**
TO6	5.10^{-6}	0.69	**31**
	10^{-5}	0.45	**55**
	10^{-4}	0.29	**71**
	2.10^{-4}	0.08	**92**

From Table 1, it can be seen that in this corrosive medium, for lower concentrations of inhibitors (10^{-6} M) the best yield is obtained with **TO1** (39%). On the other hand, for higher concentrations, the best percentage of the inhibitory performance is recorded to be 97% at 2.10^{-4} M. From the same table, it can easily be seen that the inhibitor **TO1** is the most effective. This is due to the presence of a methoxy group (positive mesomeric effect) on the structure of the molecule, and can be adsorbed in its planar form, thereby covering a maximum of the active sites.

4. 2. Polarization curves

The polarization curves have been realized with and without **TO1**, **TO4** and **TO6** at different concentrations, in 1M HCl at 30 °C. The polarization curves are represented in the Figures 2a-c, respectively.

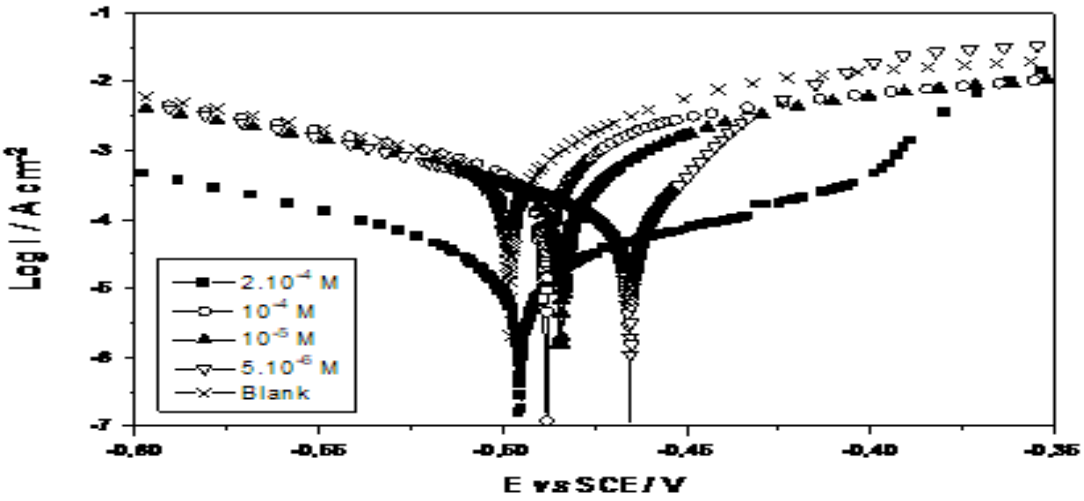

Figure 2.a. Polarization curves for C38/1M HCl system containing different concentrations of **TO1.**

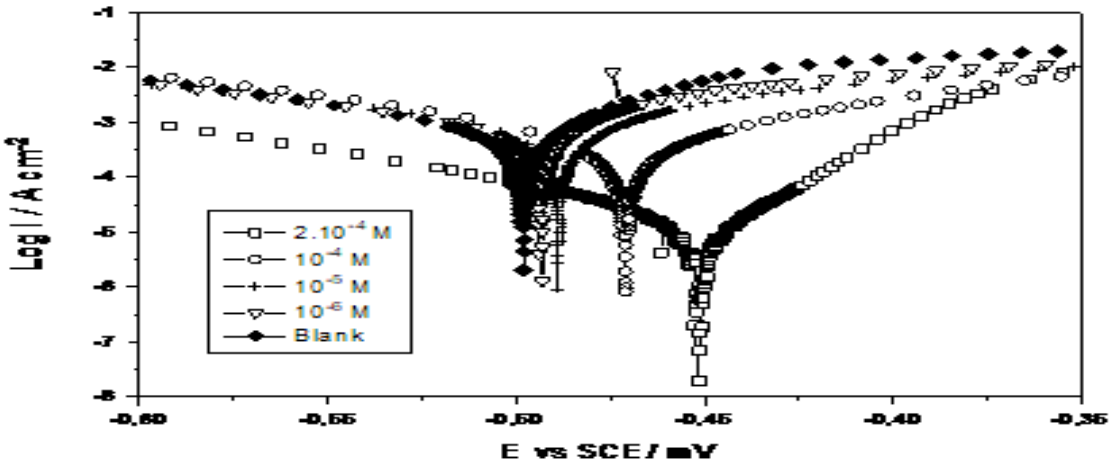

Figure 2.b. Polarization curves for C38/1M HCl system containing different concentrations of **TO4.**

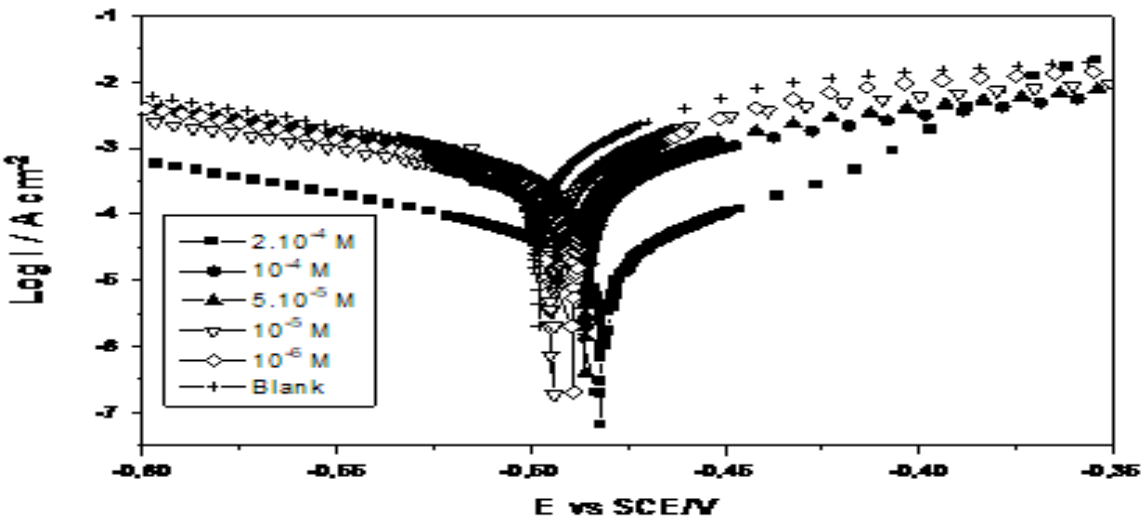

Figure 2.c. Polarization curves for C38/1M HCl system containing different concentrations of **TO6.**

In view of the curves obtained, we can clearly see that the addition of the three inhibitors reduce systematically the current densities (cathodic and anodic branches). The evolution of the LogI=f(E) curves as a function of the concentration of TO1**, TO4** and **TO6** is substantially identical. Table 2 gives the electrochemical parameters obtained from the above curves.

Table 2. Electrochemical parameters and inhibitory efficiency for different concentrations of **TO1**, **TO4** and **TO6** for corrosion of C38 steel in 1M HCl obtained by polarization curves

	Conc. (M)	**E_{corr} (mV vs SCE)**	**b_c (mV.dec^{-1})**	**I_{corr} (mA.cm^{-2})**	**EI_{Icorr} (%)**
	Blank	-498	138	1.11	----
TO1	5.10^{-6}	-485	130	0.70	**36.94**
	10^{-5}	-483	129	0.46	**55.85**
	10^{-4}	-488	34	0.23	**79.28**
	2.10^{-4}	-495	68	0.03	**97.39**
TO4	10^{-6}	-494	137	0.72	**35.13**
	10^{-5}	-488	106	0.52	**53.15**
	10^{-4}	-470	52	0.27	**75.67**
	2.10^{-4}	-466	73	0.05	**95.49**
TO6	5.10^{-6}	-488	127	0.75	**32.43**
	10^{-5}	-486	134	0.55	**50.45**
	10^{-4}	--494	109	0.29	**73.87**
	2.10^{-4}	-481	90	0.07	**93.69**

From the results obtained, we can conclude that, when the concentration of inhibitors increases, the corrosion current densities decrease. The addition of the three inhibitors slightly modifies the values of E_{corr} (<85mV) and it is noted that the inhibitory efficacy EI(%) increases with the increase in the concentration of inhibitor. The addition of three inhibitors even at low concentration (10^{-5} M) presents good inhibitory efficiencies, for example, **TO1** gives 55.85% of efficiency. Overall, the inhibitor **TO1** is more effective than the **TO4** and **TO6** inhibitors.

The cathodic branches of curves are in the form of Tafel lines reveal that the reaction of hydrogen evolution on the surface of the steel takes place according to a pure activation mechanism. The presence of the inhibitors shows a variation in the cathode slopes of Tafel (from 138 to 34 mV / dec). This is attributed to the fact that the presence of the inhibitors influences the hydrogen release reaction [19].

*3.3. Electrochemical impedance spectroscopy (**EIS**)*

EIS experiments were performed in the same way as the polarization curve measurements in the presence and absence of the three inhibitors at the open circuit potential (1h of immersion and 30 °C). The EIS Obtained spectra are shown in figures 3a-c.

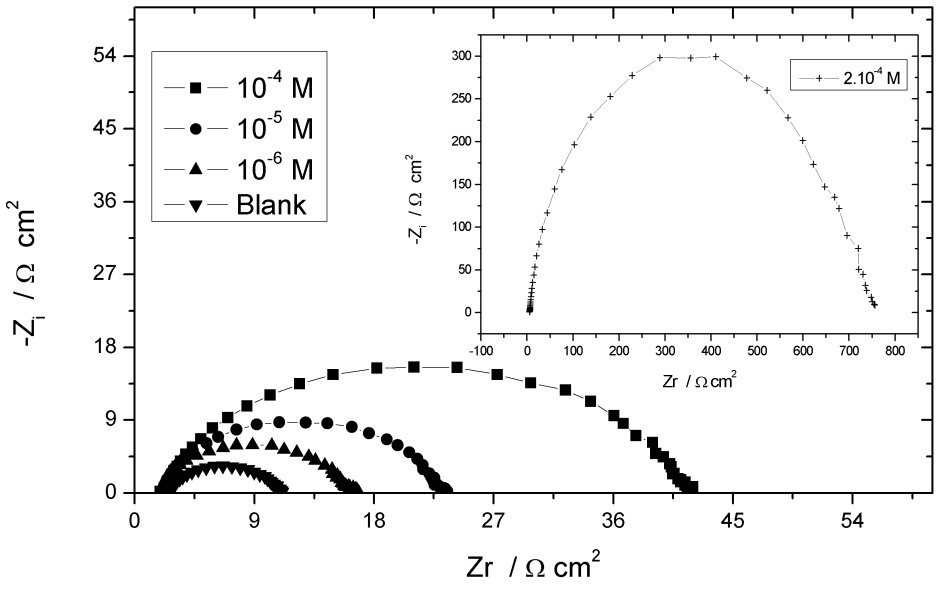

Figure 3. a. Nyquist plots for C38 steel in 1M HCl containing **TO1**

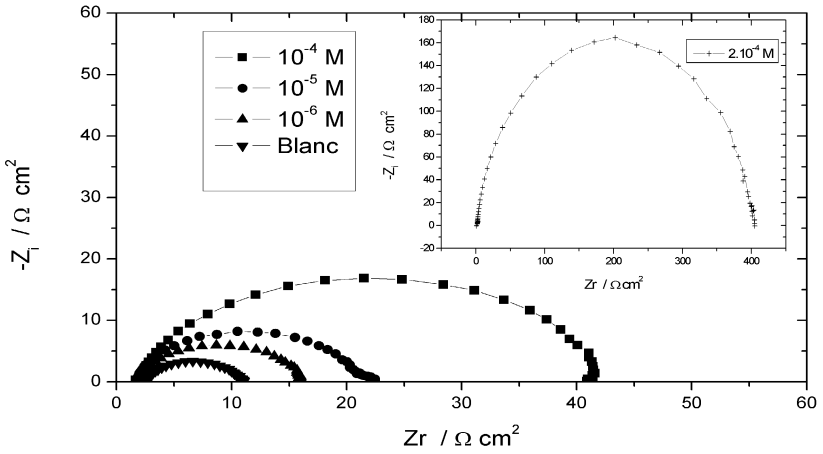

Figure 3. b. Nyquist plots for C38 steel in 1M HCl containing **TO4**

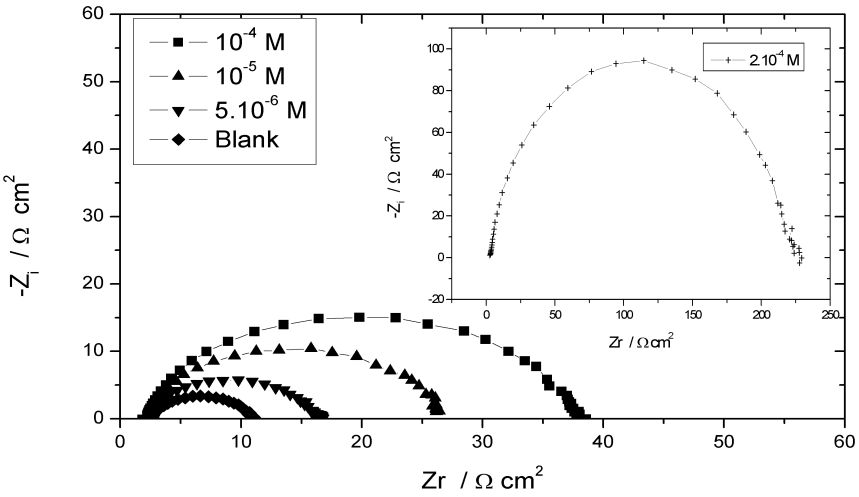

Figure 3. c. Nyquist plots for C38 steel in 1M HCl containing **TO6**

Nyquist curves show a single depressed capacitive circle for all cases (blank and with inhibitors). The Nyquist diagram of the depressive circle is characteristic to roughness and surface inhomogeneities [20]. The addition of the three inhibitors does not modify the shape of the semicircle, which indicates that the addition of inhibitor does not modify the mechanism of the corrosion reaction, but inhibits corrosion by increasing the surface coverage by the thick film of the adsorbed inhibitor as well as by decreasing the capacity of the double layer [21]. This is reflected in the fact that when the concentration of inhibitors increases, the diameter of the loops increases [22].

The electrical equivalent circuit used to calculate the inhibitory efficiencies in this part is similar to that which was described in our previous work [11, 22-24]. The obtained results are given in Table 3.

Table 3. Impedance parameters recorded for C38 steel / 1M HCl system containing **TO1**, **TO4** and **TO6** at different concentrations.

	Conc. (M)	**R_t (cm^2)**	**C_{dl} (µF cm^{-2})**	**EI $_{Rt}$(%)**
	Blank	12.5	290	**----**
TO1	5.10^{-6}	17.50	195	**28.57**
	10^{-5}	24.50	120	**48.98**
	10^{-4}	43.00	105	**70.93**
	2.10^{-4}	750.00	36	**98.33**
TO4	10^{-6}	16.50	205	**24.24**
	10^{-5}	21.50	131	**41.86**
	10^{-4}	42.00	107	**70.24**
	2.10^{-4}	405.00	46	**96.91**
TO6	5.10^{-6}	13.25	220	**22.36**
	10^{-5}	22.65	150	**51.92**
	10^{-4}	36.89	99	**66.22**
	2.10^{-4}	206.6	60	**94.44**

From the data presented in Table 3, it is clearly noted that the values of R_t increase with the concentration of **TO1**, **TO4** and **TO6** while the values of C_{dl} for the inhibitors are lower than that of the blank, which suggests as the inhibitors gradually adsorb onto the surface of the steel, thus forming a thick protective layer on the C38 steel surface and reducing the charge transfer process. Globally, the decrease in C_{dl} is attributed to a decrease in the dielectric constant and an increase in the thickness of the electric double layer, suggesting that the molecules of **TO1**, **TO4** and **TO6** are strongly adsorbed at the metal / solution interface. The calculated values of EI_{Rt} (%) are also listed in Table 3.

Consequently, these results suggest that the three products tested are effective corrosion inhibitors for C38 steel in the medium studied. Therefore, the three products tested could serve as effective corrosion inhibitors for C38 steel in 1M HCl. It should be noted that the obtained results by the above used methods are reasonably in good agreement.

3.4. Adsorption isotherm

The obtained results by electrochemical impedance spectroscopy method are used to calculate the surface coverage ($\Theta = E.I/100$).

The Langmuir isotherm gives the best fit (where, C is the inhibitors concentration and K is the equilibrium constant of adsorption).

Indeed, linear straight lines have been obtained with a slope very close to unity (Figure 4).

It should be noted that this isotherm implies the hypothesis of the absence of interaction between the species adsorbed on the surface of the steel and that there exists a fixed number of energy identical sites. Each site can only adsorb one particle [25].

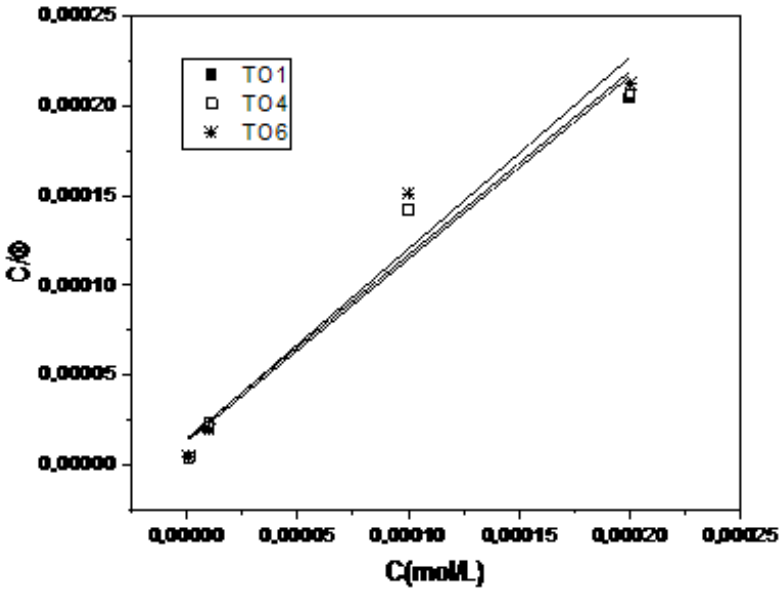

Figure 4. Adsorption isotherm plot of C38 steel /1 M HCl system in presence of **TO1**, **TO4** and **TO6**.

The ΔG_{ads} is given by:

$$K = 55.5 \exp(-\Delta G_{ads}/RT) \quad (5)$$

where K is equilibrium constant of adsorption, R = 8.314 J/mol. K and T is temperature in Kelvin).
The thermodynamic parameters obtained by the Langmuir adsorption isothrem are listed in Table 4.

Table 4. Obtained thermodynamic parameters of adsorption for **TO1**, **TO4** and **TO6**.

Inhibitor	1/K (Mol/L)	Slope	ΔG_{ads} (kJ/mol)
TO1	7.63 x 10^4	1.01	**-39.07**
TO4	6.76 x 10^4	1.01	**-38.76**
TO6	6.59x 10^4	1.06	**-38.69**

The calculated free energy ΔG^0_{ads} values are around -39 kJ / mol (Table 4). These results indicate that the adsorption mechanism of **TO1**, **TO4** and **TO6** inhibitors on the surface involves two types of adsorption (physisorption with a tendency to chemisorption) [26]. Extensive details on the types of adsorption as well as the processes involved have been well detailed in our published works [19, 27].

3.5. Analysis of the organic film formed by XPS photoelectron spectroscopy

The presence of thiazole compounds on the surface of the steel was detected based on the signal characteristic of the atom of sulfur S2p and nitrogen N1s. The XPS spectra were obtained for the surface of the steel immersed for 24 h at 30 °C in 1M HCl in the presence of 2.10^{-4} M of **TO1**. For comparative purposes, the XPS spectrum of pure TO1 was also performed.

The S2p spectra of pure **TO1** (figures 5.a-d) and of the steel treated in HCl 1M are given in Figure 6a-d. The peak obtained for the pure compound at 164.3 eV can be attributed to the structure –S– [28], and the peak observed at 161 eV has the structure C=S [29]. These structures -S- and C=S are found on the surface of the steel treated with HCl with the appearance of new peaks at 161 eV and 168 eV.

Based on the deconvolution of the S2p spectrum of the treated surface, presented in Figure 6a, we can see that sulfur appears in four chemical states. These correspond to the –S– form (163 eV and 163.5 eV), C=S (161.5 eV and 161, 7 eV) [29] and to the S–Fe form (161 eV and 161.1 eV) [30].

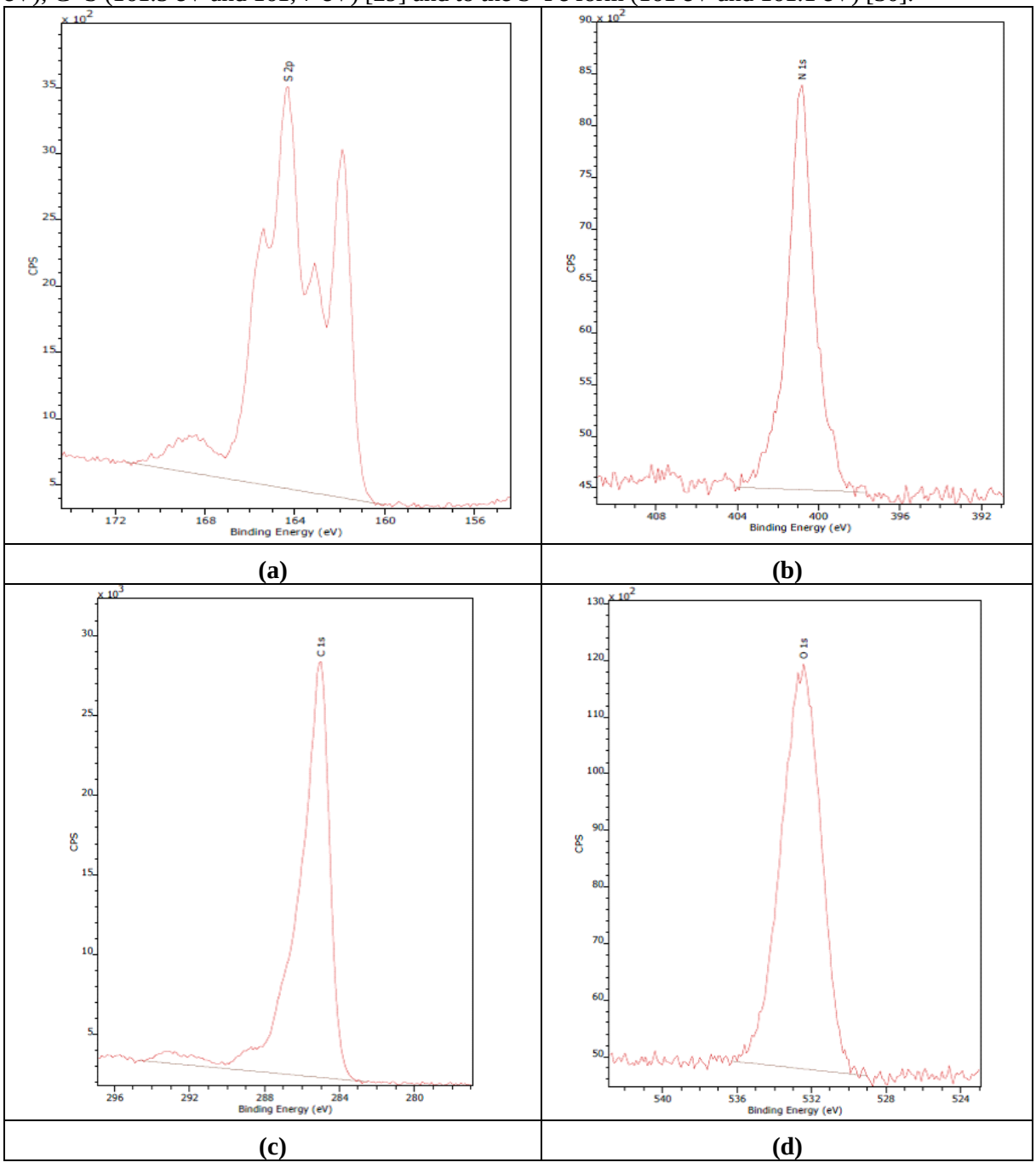

Figure 5. XPS spectra of (a)S 2p, (b) N 1s, (c) C 1s and (d)O 1s for pure **TO1**.

Concerning nitrogen, analysis of the N1s spectrum of the pure compound (Figure 5b) shows the existence of a single peak centered at 400.8 eV corresponding to the structure –N.

The deconvolution of the spectrum N1s of the sample TO1 on the inhibited surface, gives three components (figure 6 b), a majority attributed to the form –N (400 eV et 400,1 eV) **[40],** the second observed at (397.8 eV and 399.6 eV) can be attributed to nitrogen adsorbed on the metal surface (N-Fe) [31] and the last at 401.7 eV and 401.8 eV is assigned to nitrogen positively charged (> N^+–) [32].

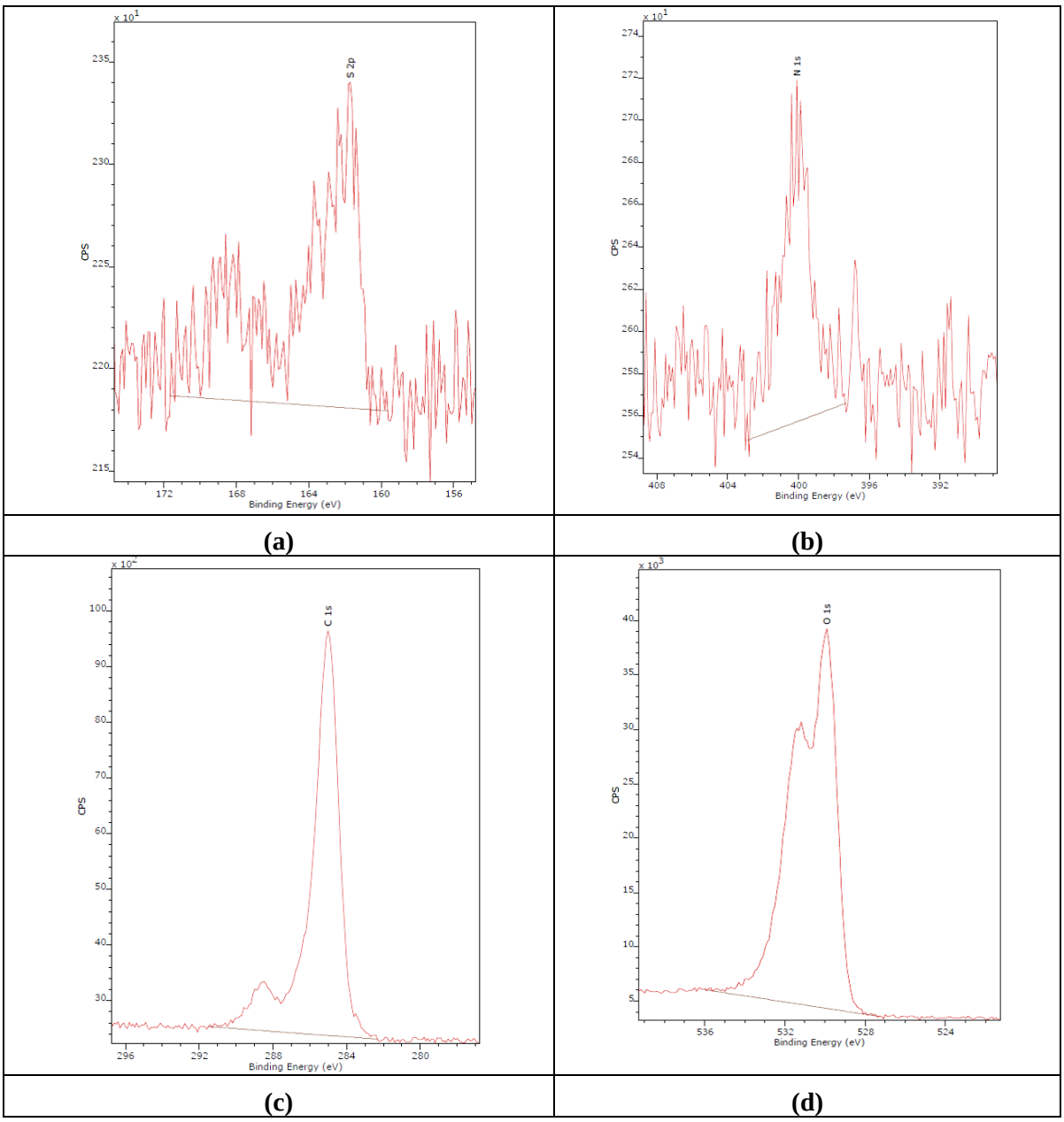

Figure 6. XPS spectra of (a) S 2p, (b) N 1s, (c) C 1s and (d) O 1s for C38 steel treated by **TO1** in HCl 1M

The XPS C 1s spectrum of pure **TO1** has a peak at 285 eV and another at 288.5 eV, moreover in the C1s spectrum of the surface protected in HCl, three signal peaks of element C were observed. The binding energy of 284.6 eV corresponding to the structures C–C and C–H, while the binding energies

of 286.2 eV and 288.1 eV are assigned to C–S / C–N and C=S, respectively [30, 33-34]. The values of different picks are illustrated in the table 5.

The spectra of O1s demonstrate that O exists mainly in FeOOH, Fe_2O_3 and Fe_3O_4 [30, 32]. The 529.9 eV signal assigned to the O^{-2} structure, linked to Fe oxide in Fe_2O_3 and Fe_3O_4 while the 531.1 eV signal is linked to OH^- in FeOOH. The presence of Fe_2O_3 and Fe_3O_4 could be the consequence of the oxidation of the sample in the air before the XPS test [34-35].

Studies on Fe2p make it possible to detect Fe-S bond peaks at 709.8 eV, indicating the formation of bonds between the sulfur atom S present in the molecules of **TO1** and Fe **[**36]. The signal intensity of Fe-S is significant, indicating that the adsorption of **TO1** on the surface of Fe is important [30].

The XPS spectrum of the surface of the steel covered by the chemisorbed **TO1** molecules (Figure 7) reveals the existence of a binding energy component at 711 eV (Fe2p3/2) and at 724 eV (Fe 2p1/2) characteristic of Fe^{3+} and Fe^{3+}, showing the oxidation of the steel surface [37]. The increased signal of Fe2p confirms adsorption and film formation on the surface of the steel [30].

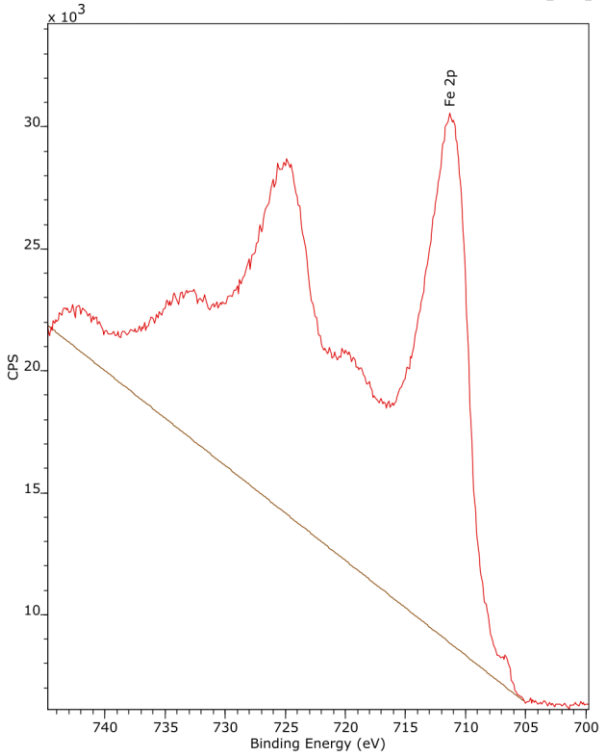

Figure 7. XPS spectra of Fe2p3/2 and Fe 2p1/2 for C38 steel treated by **TO1** in HCl 1M.

Globally, these XPS studies clearly show that the products **TO1** are strongly adsorbed (chemisorption with a predomination of physisorption) on the surface of C38 steel, and that the structures of organic inhibitors are modified, the adsorption mechanism of these three products is therefore essentially based on a charge transfer between the organic inhibitor and the steel surface in 1M HCl [38].

3.6. Adsorption mechanism

Based on the processing of the XPS results, we can propose the following adsorption mechanisms: the molecules of **TO1**, **TO4** and **TO6** are protonated at the level of the nitrogen atom (N) (product (II) in Figure 7). Moreover, in an acid medium such as 1M HCl, the surface of the steel is positively charged [34]. Thus, the Cl^- ions are the first to be adsorbed on the metal surface and we will have the adsorption

of the cationic forms of the three inhibitors (Figure 7) electrostatically via the adsorbed chloride [39-40].

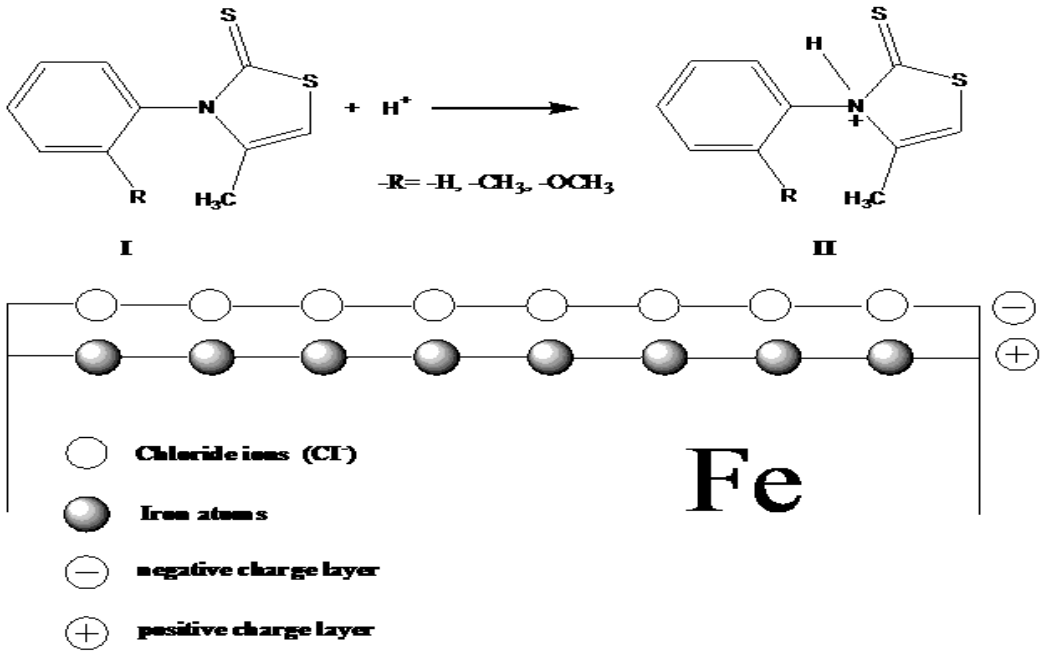

Figure 7. Adsorption mechanism of **TO1**, **TO4** and **TO6** on a C38 steel surface in 1M HCl with formation of thiazolium cation

In a second imaginative case of chemisorption, the three inhibitor molecules can be adsorbed via donor-acceptor interactions (formation of dative covalent bonds) between the electrons of the aromatic rings and unshared electron pairs of heteroatoms (N, S) with empty orbitals of metal atoms, leading to the formation of a stable chemisorbed protective film [41]. This effect is reinforced by the capacity of the substituents (-CH_3) and (-OCH_3) electron donor group of the aromatic nucleus in these thiazolinethione derivatives, as illustrated in Figure 8, resulting in the nitrogen atoms of the 1,3-thiazole ring being found with an excess of negative charges. It should be noted that the combination of the two types of adsorption clearly improves the adsorption of inhibitor molecules on the metal surface. In addition, **TO1** has a favorable geometry by contribution to the two other inhibitors **TO4** and **TO6** which can explain its better adsorption and consequently its inhibitory capacity slightly superior by contribution to the two other tested products **TO4** and **TO6**.

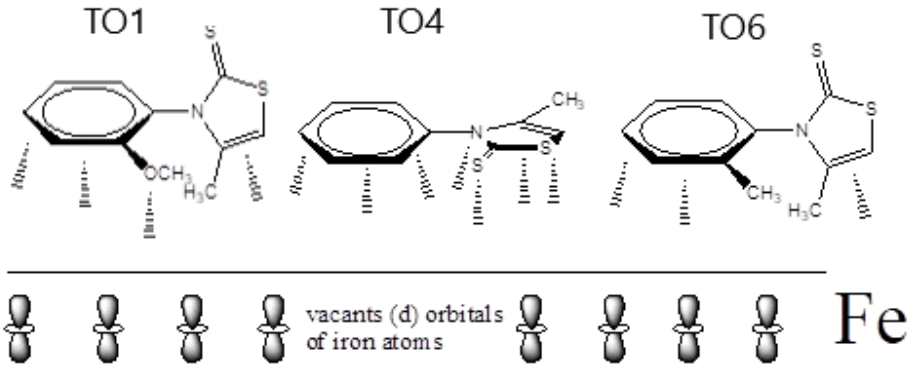

Figure 8. TO1, **TO4** and **TO6** adsorption mechanism on a C38 steel surface.

Indeed, the product **TO6** has a coplanar geometry (prevention of free rotation) between the two cycles, the aromatic nucleus and the thiazole cycle because of the interaction and the steric hidrance caused by the substituents (-CH_3) of the aromatic nucleus in ortho position and the (-CH_3) of thiazolinethione, this phenomenon is called atropisomerism [42-43]. On the other hand in **TO1** the two cycles, aromatic and thiazolinethione are reinforced by the presence of the **OMe** group. Globally, presence of group with donor mesomeric effect like the methoxy group gives to the molecule a great delocalization of the n and π electrons in the inhibitor molecule, hence the possibility of having a strong fixation on the surface of the metal.

3.7. Quantum Chemical Calculation

In order to study the correlation between inhibition efficiencies and structures of **TO1**, **TO4** and **TO6**, and complement the experimental investigation, quantum chemical calculations have been performed [44-45]. In this context, density functional theory (DFT) has been strongly used to investigate and understand the adsorption and inhibition mechanism in the corrosion process [46].

Popular qualitative chemical concepts like E_{HOMO}, E_{LUMO}, energy gap (ΔE), dipole moment (μ), absolute electronegativity (χ), ionization potential (IP), electron affinity (EA), global hardness (η), softness(σ), global electrophilicity index (ω) and fraction of transferred electrons (ΔN) of the inhibitors are presented in Table 5. The following equations allow to calculate [47]:

$$IP = -E_{HOMO}$$

$$EA = -E_{LUMO}$$

$$\Delta E = E_{LUMO} - E_{HOMO} = IP - EA$$

$$\chi = \frac{IP+EA}{2}$$

$$\eta = \frac{IP-EA}{2}$$

$$\sigma = \frac{1}{\eta}$$

$$\omega = \frac{\mu^2}{2\eta}$$

$$\Delta N = \frac{\chi_{Fe} - \chi_{inh}}{2(\eta_{Fe} + \eta_{inh})}$$

To calculate ΔN, the used values: χ_{Fe} =7.0 eV and η_{Fe} = 0.

The electron density distributions (HOMO and LUMO) of the three inhibitors are shown in Fig. 10 and the quantum chemical parameters are presented in Table 7.

Inhibitor	HOMO	LUMO
TO1	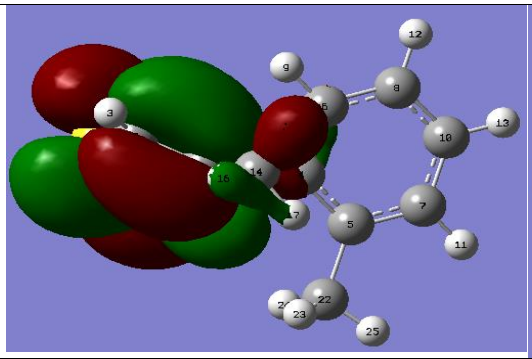	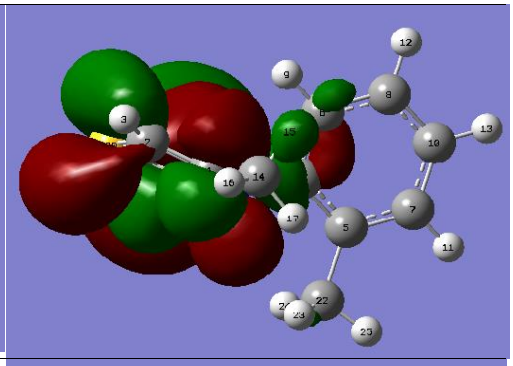
TO4	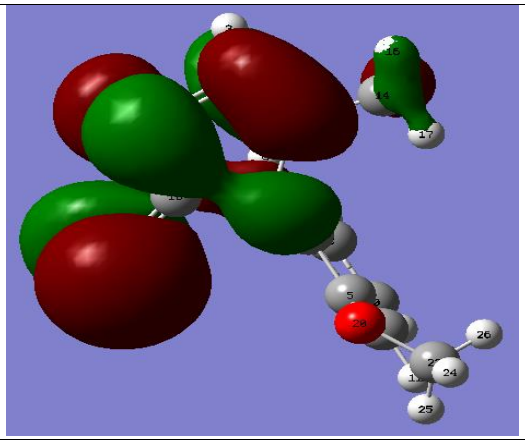	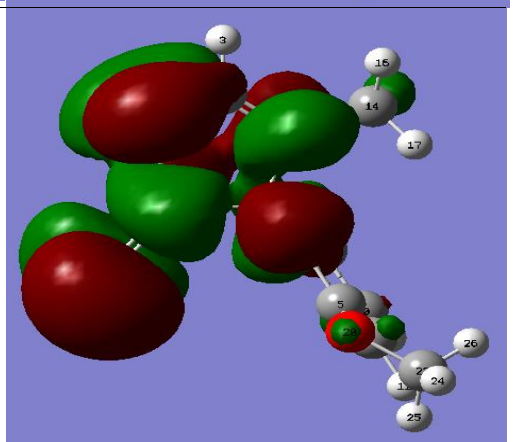
TO6	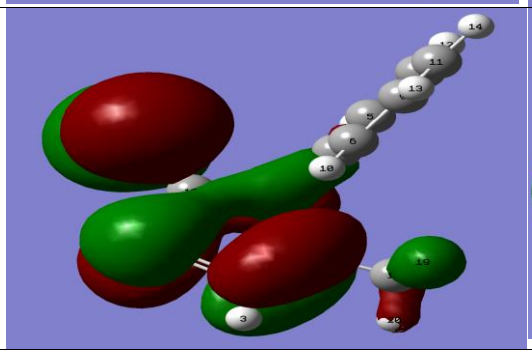	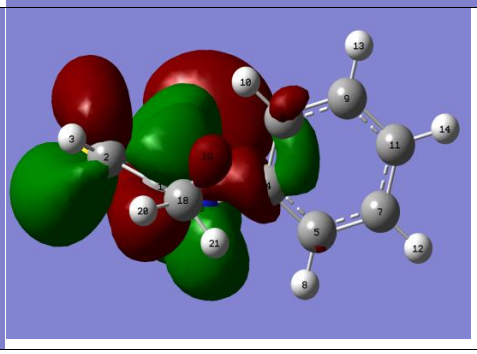

Figure 10. Molecular orbitals (HOMO and LUMO) for **TO1**, **TO4** and **TO6**.

The E_{HOMO} often describes the electron donating ability of a molecule [48].The higher the value of E_{HOMO} of an inhibitor, the greater is its ability of donating electrons to unoccupied d-orbital of the metal atoms. In contrast, the E_{LUMO} denotes the tendency of a molecule to accept electrons, the lower the value of E_{LUMO}, and the greater is its ability of the molecules to accept electrons from metal surface [49]. It can clearly be seen in Figure 9 that the electron of the density distribution of HOMO and LUMO is located on the methoxy group and the thiazole aromatic rings indicating that these segments are the preferred active sites for adsorption of TO1. Therefore, the energy difference ΔE is among the important factors related to the reactivity of a molecule and their attachment to the metal surface. Moreover, an inhibitor having a very low ΔE value is easily polarizable, i.e. that the passage of electrons from the last occupied orbital to the unoccupied molecular orbital requires little energy[50].

Table 5. Quantum chemical descriptors for **TO1**, **TO4** and **TO6** inhibitors calculated using B3LYP/6-31G (d,p).

Inhibitors	**TO1**	**TO4**	**TO6**
E_{HOMO} (eV)	-5.222	-5.390	-5.398
E_{LUMO} (eV)	-0.647	-0.810	-0.785
ΔE (eV)	4.575	4.580	4.613
μ (D)	6.336	5.965	5.771
I.P. (eV)	5.222	5.390	5.398
E.A. (eV)	0.647	0.810	0.785
Electronegativity (χ) (eV)	2.934	3.100	3.092
Global hardness (η) (eV)	2.288	2.290	2.307
Goftness (σ)	0.437	0.4366	0,4335
Global electrophilicity index (ω)	8.773	7.766	7.218
Fraction of transferred electrons (ΔN)	0,888	0,851	0,847

Table 5 shows that the TO1 has the lowest hardness (2.288 eV) and the highest softness (0.437 eV) values. Ionization potential (IP) is a fundamental descriptor of the chemical reactivity of atoms and molecules. High IP value indicates high stability and chemical inertness and small IP value indicates high reactivity of the atoms and molecules [47]. The low IP value (5.222 eV) of **TO1** indicates the high inhibition efficiency. Absolute hardness and softness are important properties to measure the molecular stability and reactivity. It is apparent that the chemical hardness fundamentally signifies the resistance towards the deformation or polarization of the electron cloud of the atoms, ions or molecules under small perturbation of chemical reaction. A hard molecule has a large energy gap and a soft molecule has a small energy gap [47]. In this **TO1** with low hardness value 2.288eV compared with **TO4** and **TO6**, have a low energy gap.

According to Sanderson's electronegativity equalization principle [51], TO1 with a high electronegativity quickly reaches equalization and hence high reactivity is expected which in turn indicates high inhibition efficiency. The electrophilicity index, ω, shows the ability of the inhibitor molecules to accept electrons. It is a measure of the stabilization in energy after a system accepts additional amount of electron charge from the environment [52]. In our present study, **TO6** is the strongest nucleophile while **TO1** is the strongest electrophile. The number of electrons transferred (ΔN) was also calculated and tabulated in Table 3. Values of ΔN show that the inhibition efficiency resulting from electron donation agree with Lukovits's study [53]. If $\Delta N < 3.6$, the inhibition efficiency increases by increasing electron-donating ability of these inhibitors to donate electrons to the metal surface and it increases in the following order: **TO1>TO4>TO6**. The results indicate that ΔN values correlates strongly with experimental inhibition efficiencies. Thus, the highest reaction of electrons transferred is associated with the best inhibitor (**TO1**).

4.Conclusion

From the results of the study the following may be concluded:

- Both investigated compounds are efficient corrosion inhibitors for C38 steel in 1 M HCl solution.
- The effectiveness of these inhibitors depends on their structures. The order of % IE of these investigated compounds is the following: TO1 >TO4>TO6.
- The results obtained from polarization curves indicated that the investigated compounds are mixed type inhibitors.
- The EIS results confirm that the addition of inhibitors to the aggressive solution results in an increase in R_{ct} and a decrease in C_{dl}.
- The mode of adsorption follows Langmuir isotherm, suggesting a nature of simultaneous physisorption and chemisorption.
- The inhibition efficiencies calculated from the three methods (weight loss, polarization and electrochemical impedance measurements) are in good agreement.
- The presence of the protective layer formed on the surface of the carbon steel was confirmed by XPS.
- Theoretical studies confirm the results of experimental studies.
-

References

1. C. Verma, L.O. Olasunkanmi, I.B. Obot, E.E. Ebenso, M.A. Quraishi, RSC Adv., 6 (2016) 53933–53948

2. Y. Sasikumar, A.S. Adekunle, L.O. Olasunkanmi, I.R. Bahadur Baskar, M.M. Kabanda, I.B. Obot, E.E. Ebenso, J. Mol. Liq., 211(2015)105–118

3. S.K. Ahmed, W.B. Ali, A.A. Khadom, Inter. J. Ind. Chem., 10 (2019) 159–173.

4. F. Fadel, D. Ben Hmamou, R. Salghi, B. Chebli, O. Benali, A. Zarrouk, E.E. Ebenso, A. Chakir, B. Hammouti, Inter. J. Electrochem. Sci., 82013 (2013) 11019-11032.

5. H.B. Ouici, M. Tourabi, O. Benali, C. Selles, M. Traisnel, C. Jama, F. Bentiss, R. Salghi, J. Mater. Environm. Sci. 7(8) (2016) 2971-2988.

6. H.B. Ouici, O. Benali, A. Guendouzi, Res. Chem. Intermed., 42 (9) (2016) 7085-7109.

7. F. Chaib,· H. Allali, O. Benali, G. Flamini, Int. J. Chem. Biochem. Sci., 18 (2020) 129-136.

8. A. Attou, A. Benikdess, O. Benali, H.B. Ouici, A. Guendouzi, Int. J. Chem. Biochem. Sci., 17 (2020) 120-128.

9. A. Attou, M. Tourabi, A. Benikdes, O. Benali, H.B. Ouici, F. Benhiba, A. Zarrouk, C. Jama, F. Bentiss, Coll. Surf. A: Physicochemi. Eng. Aspc., 604 (2020) 125320.

10. A. Sehmi, H.B. Ouici, A. Guendouzi, M. Ferhat, O. Benali, F. Boudjellal, J. Electrochem. Soc., 167 (2020) 155508.

11. H.B. Ouici, M. Tourabi, O. Benali, C. Selles, C. Jama, A. Zerrouk, F. Bentiss, J. Electroanal. Chem., 803 (2017) 125-134.

12. O. Benali, A. Benikdes, D. Ben Hmamou, Pharmac. Chem. J., 7(3) (2020)56-68.

13. M. Hegde, S.P. Nayak, J. Chem. Pharm. Sci., 1 (2018) 16-24.

14. M. Zebida, O. Benali, U. Maschke, M. Trainsel, Inter. J. Corros. Scale. Inhib., 8(3) (2019) 613–627.

15. C. Roussel, M. Adjimi, A. Chemlal, A. Djafri, J. Org. Chem., 53 (1988) 5076-5080.
16. C. Roussel, F. Andreoli, M. Roman, M. Hristova, N. Vanthuyne, Molecules, 10 (2005) 327–333.
17. Gaussian 09, Revision, A. 1, M.J. Frisch, G.W. Trucks, H.B. Schlegel, G.E. Scuseria, M.A. Robb, J.R. Cheeseman, G. Scalmani, V. Barone, B. Mennucci, G.A. Petersson, H. Nakatsuji, M. Caricato, X. Li, H.P. Hratchian, A.F. Izmaylov, J. Bloino, G. Zheng, J.L. Sonnenberg, M. Hada, M. Ehara, K. Toyota, R. Fukuda, J. Hasegawa, M. Ishida, T. Nakajima, Y. Honda, O. Kitao, H. Nakai, T. Vreven, J.A. Montgomery Jr., J.E. Peralta, F. Ogliaro, M. Bearpark, J.J. Heyd, E. Brothers, K.N. Kudin, V.N. Staroverov, R. Kobayashi, J. Normand, K. Raghavachari, A. Rendell, J.C. Burant, S.S. Iyengar, J. Tomasi, M. Cossi, N. Rega, J.M. Millam, M. Klene, J.E. Knox, J.B. Cross, V. Bakken, C. Adamo, J. Jaramillo, R. Gomperts, R.E. Stratmann, O. Yazyev, A.J. Austin, R. Cammi, C. Pomelli, J.W. Ochterski, R.L. Martin, K. Morokuma, V.G. Zakrzewski, G.A. Voth, P. Salvador, J.J. Dannenberg, S. Dapprich, A.D. Daniels, O. Farkas, J.B. Foresman, J.V. Ortiz, J. Cioslowski, D.J. Fox, Gaussian, Inc., Wallingford CT, 2009.
18. A.D. Becke, J. Chem. Phys. 98 (1993) 1372-1377.
19. O. Benali, L. Larabi, B. Tabti, Y. Harek, Anti-Corros Meth. Mater., 52 (2005) 280.
20. I.D. Raistrick, D.R. Franceschetti, J.R. Macdonald, Impedance spectroscopy, in:E. Barsoukov, J.R. Macdonald (Eds.), Theory, Experimental and Applications, (2005) second ed., John Wiley & Sons, New Jerse.
21. T. Zhihua, Z. Shengtao, L. Weihua, H. Baorong, Ind. Eng. Chem. Res., 50 (2011) 6082–6088.
22. M. Mahdavian, S. Ashhari, Electrochim. Acta, 55 (2010)1720–1724.
23. H.B. Ouici, O. Benali, Y. Harek, L. Larabi, B. Hammouti, A. Guendouzi, Res. Chem. Intermed., 39 (2013) 2777–2793.
24. H.B. Ouici, O. Benali, Y. Harek, S.S. Al-Deyab, L. Larabi, B. Hammouti, Int. J. Electrochem. Sci., 7 (2012) 2304- 2319.
25. M. Elayyachy, A. El Idrissi, B. Hammouti, Corros. Sci., 48 (2006) 2470–2479.
26. A.K. Singh, B. Chugh , S.Kr. Saha, P. Banerjee, E.E. Ebenso, S. Thakur, B. Pani, Res. Phys., 14 (2019) 102383.
27. O. Benali, L. Larabi, S. M. Mekelleche, Y. Harek, J. Mater. Sci., 41 (2006) 7064–7073.
28. R. Riga, J.J. Verbist, J. Chem. Soc. Perklin Trans. II, (1983) 1545.
29. C. Cauletti, L. Sestili, R. Zanoni, Inorg. Chim. Acta; 147 (1988) 231-242.
30. H. Cen, J. Cao, Z. Chen, X. Guo, Appl. Surf. Sci., 476 (2019) 422-434.
31. K.L. Tan, B.T.G. Tan, E.T. Kang, K.G. Neoh, J. Mater. Sci. 27(1992) 4056.
32. P. Shaw, I. B. Obot, M. Yadav, Mater. Chem. Front., 3 (2019) 931-940.
33. O. Olivares-Xometl, N. V. Likhanova, R. Martínez-Palou, M. A. Domínguez-Aguilar, Mater. Corros., 60 (2009) 14-21.
34. A. Zarrouk, B. Hammouti, T. Lakhlifi, M. Traisnel, H. Vezin, F. Bentiss, Corros. Sci., 90 (2015) 572-584.
35. N.Z. Nor Hashim, E. Anouar, K. Kassim, H.M. Zaki, A.I. Alharthi, Z. Embong, Appl. Surf. Sci., 476 (2019) 861-877.
36. L Wei, X Pang, C Liu, K Gao, Corros Sci. 100 (2015) 404-420.
37. Y Hua, R Barker, A Neville, Appl. Surf. Sci., 356 (2015) 499-511.

38. M. Tourabi, K. Nohair, M. Traisnel, J. Jama, F. Bentiss, Corros. Sci., 75 (2013) 123–133.
39. W. Gong, X. Yin, Y. Liu, Y. Chen, W. Yang, Prog. Org. Coat., 126 (2019) 150–161.
40. N. Yilmaz, A. Fitoz, Ü. Ergun, K.C. Emregül, Corros. Sci., 111 (2016) 110–120.
41. M. Corrales-Luna, T. Le Manh, M. Romero-Romo, M. Palomar-Pardavé, E.M. Arce-Estrada, Corros. Sci., 153(2019) 85-99.
42. F. Andreoli, R. Kaid-Slimane, F. Coppola, D. Farran, N. Vanthuyne, C. Roussel, J. Org. Chem., 80 (6) (2015) :3233-3241.
43. H. Leopold, A. Tronnier, G. Wagenblast, I. Münster, T. Strassner, Organometallics, 35(7) (2016) 959-971.
44. M.A. Abuelela, M.A. Bedair, W.M. Zoghaib, L.D. Wilson, T.A. Mohamed , J. Mol. Struct., 1230 (2021) 129647
45. A. El Aatiaoui, M. Koudad, T. Chelfi, S. Erkan, M. Azzouzi, A. Aouniti, K. Savas, M. Kaddouri, N. Benchat, A. Oussaid, J. Mol. Struct., 1226 (2021) 129372
46. I. Selatnia, A. Sid, M. Benahmed, O. Dammene debbih, T. Ozturk, N. Gherraf, Protec. Met. Phys. Chem. Surf., 54 (6) (2018) 1182–1193.
47. *M*. Yadav, *D.* Behera, *S.* Kumar, *R.R.* Sinha, Indian J. Chem. Techn. 21(4) (2014) 249-256.
48. H.M. Abd El-Lateef, A.M. Abu-Dief, L.H. Abdel-Rahman, E.C. Sañudo, N. Aliaga-Alcalde, J. Electroanal. Chem., 743 (2015) 120-133.
49. G. Gece, Corros. Sci., 50 (11) (2008) 2981-2992.
50. N.M. El Basiony, E.H. Tawfik, M. Abd El-raouf, A.A. Fadda, M.M. Waly, J. Mol. Struct., 1231 (2021) 129999.
51. P. Geerlings, F. De Proft, Int. J. Mol. Sci., 3 (2002) 276-309.
52. S. Liu, J. Chem. Sci., 117 (5) (2005) 477-483.
53. I. Lukovits, E. Kalman, F.Zucchi, Corrosion, 57 (2001) 3-8.